Title

Self-reinforcing loop of amphiregulin and Y-box binding protein-1 contributes to poor outcomes in ovarian cancer

Journal

Oncogene, 33(22)

ISSN

0950-9232

Authors

Panupinthu, N
Yu, S
Zhang, D
et al.

Publication Date

2014-05-29

DOI

10.1038/onc.2013.259

Peer reviewed

Published in final edited form as:
Oncogene. 2014 May 29; 33(22): 2846–2856. doi:10.1038/onc.2013.259.

Self-reinforcing loop of amphiregulin and Y-box binding protein-1 contributes to poor outcomes in ovarian cancer

Nattapon Panupinthu[1,3], **Shuangxing Yu**[1], **Dong Zhang**[1], **Fan Zhang**[1], **Mihai Gagae**[2], **Yiling Lu**[1], **Jennifer R. Grandis**[4], **Sandra E. Dunn**[5], **Hoi Young Lee**[6], and **Gordon B. Mills**[1]

[1]Department of Systems Biology, The University of Texas MD Anderson Cancer Center, Houston, TX, 77030, USA [2]Department of Veterinary Medicine & Surgery, The University of Texas MD Anderson Cancer Center, Houston, TX, 77030, USA [3]Department of Physiology, Faculty of Science, Mahidol University, Bangkok, 10400, Thailand [4]Department of Otolaryngology and Department of Pharmacology and Chemical Biology, University of Pittsburgh, Pittsburgh, PA, 15213, USA [5]Departments of Pediatrics and Experimental Medicine, Child and Family Research Institute, University of British Columbia, Vancouver, BC, V5Z 4H4, Canada [6]Department of Pharmacology, College of Medicine, Konyang University, Daejeon, 302-718, Republic of Korea

Abstract

The Y-box binding protein-1 (YB-1) transcription factor is associated with unfavorable clinical outcomes. However, the mechanisms underlying this association remain to be fully elucidated. We demonstrate that YB-1 phosphorylation, indicative of YB-1 activation, is a powerful marker of outcomes for ovarian cancer patients. In ovarian cancer, YB-1 phosphorylation is induced by activation of the lysophosphatidic acid (LPA) receptor (LPAR) via SRC-dependent transactivation of the epidermal growth factor receptor (EGFR) that is coupled to MAPK/p90 ribosomal S6 kinase (p90RSK), but not phosphatidylinositol 3-kinase (PI3K)/AKT signaling. Activation of the LPAR/SRC/EGFR/MAPK/p90RSK/YB-1 axis leads to production of the EGFR ligand amphiregulin (AREG). AREG induces ongoing YB-1 phosphorylation as well as YB-1-dependent *AREG* expression thus constituting an AREG/YB-1 self-reinforcing loop. Disruption of transactivation of the EGFR and the downstream self-reinforcing loop decreases invasiveness of ovarian cancer cells *in vitro* and limits ovarian cancer growth in xenograft models. These findings established the regulation and significance of YB-1 phosphorylation, therefore further exploration of this signaling axis as a therapeutic avenue in ovarian cancer is warranted.

Keywords

Autoregulation; Crosstalk; Feedback; G-protein-coupled receptor; Receptor tyrosine kinase

Corresponding Author: Nattapon Panupinthu, PhD Department of Physiology Faculty of Science Mahidol University 272 Rama VI Road, Ratchathewi District Bangkok, Thailand, 10400 Tel: +66 2201 5610 Fax: +66 2354 7154 npanupin@gmail.com.

CONFLICT OF INTEREST
All authors declare no conflict of interest.

INTRODUCTION

Ovarian cancer is the fifth leading cause of cancer death in women. In 2013 in the United States alone, a total of 22,240 new cases are expected with ~70 % of the patients (14,030 cases) expected to die of their disease {Siegel, 2013 #114}. This abysmal outcome is due to delayed diagnosis accompanied with extensive metastasis and limited response to therapy {Clarke-Pearson, 2009 #82}. Unfortunately, genomic characterization reported so far has failed to identify frequent targets for high-grade serous ovarian cancers, the main cause of mortality, other than *TP53* and the homologous recombination pathway {Cancer Genome Atlas Research, 2011 #79;Chetrit, 2008 #78;Jones, 2012 #62}. Therefore, further studies are needed to identify new therapeutic targets in ovarian cancer.

Studies from our laboratory and others have identified LPA (1-acyl-2-lyso-*sn*-glycero-3-phosphate) as a key growth factor in ascitic fluid, which reflects the microenvironment for ovarian cancer cell growth {Okita, 1997 #110;Xu, 1995 #104}. LPA is produced in proximity to the tumor cell by hydrolysis of lysophosphatidylcholine by cell-associated autotaxin {Tabchy, 2011 #106;Umezu-Goto, 2002 #105}. The resulting LPA binds to cell-surface G-protein-coupled LPA receptors (LPAR) to promote cancer cell functions {Mills, 2003 #111}. Importantly, enforcing the expression of the LPA2 or LPA3 receptors enhances tumorigenicity and aggressiveness of ovarian cancer cells {Yu, 2008 #103}, suggesting that LPA contributes to the pathophysiology of ovarian cancer through an autocrine LPA signaling loop.

The YB-1 transcription factor has emerged as a promising therapeutic target due to its association with advanced tumor grades and unfavorable outcomes in multiple cancer lineages {Lasham, 2012 #67}. In ovarian cancer patients, nuclear YB-1 is associated with poor outcomes and resistance to chemotherapy {Basaki, 2007 #85;Kamura, 1999 #81;Yahata, 2002 #86}. Particularly, YB-1 phosphorylation at serine-102 regulates nuclear translocation and functional outcomes of YB-1 {Stratford, 2008 #102;Sutherland, 2005 #99}. However, the clinical relevance of elevated phospho-YB-1 levels remains unknown. Moreover, the mechanism underlying YB-1 phosphorylation is not well understood. Interestingly, YB-1 was found to promote growth and aggressiveness of human mammary epithelial cells via constitutive activation of the EGFR pathway {Berquin, 2005 #84} suggesting that the association of YB-1 with poor outcomes could be due to autocrine regulation of growth factors.

In this study, we employed an integrated approach to determine the significance of YB-1 and its regulation by growth factors in ovarian cancer. Our results reveal YB-1 as a convergent hub for LPA and EGF signaling via EGFR transactivation. We provide further evidence for an unexpected model wherein YB-1 phosphorylation initiates a self-reinforcing loop involving production and release of the EGFR ligand, AREG, leading to further phosphorylation and activation of YB-1. The crosstalk and self-reinforcing loop are required for LPA-induced invasion of ovarian cancer cells. Further, an intact LPAR/EGFR/YB-1/AREG cascade is required for LPA-induced tumor growth *in vivo*.

RESULTS

YB-1 levels and phosphorylation status correlate with poor outcome of ovarian cancer patients

We began the study by establishing an association of YB-1 and patient outcomes in ovarian cancer. Our analyses from two independent ovarian cancer datasets (see Materials and Methods for sample information) revealed that expression of *YBX1* mRNA was significantly upregulated in ovarian cancers compared to normal tissues analyzed from The Cancer Genome Atlas (TCGA) dataset (http://cancergenome.nih.gov) as well as in malignant compared to low malignant potential tumors analyzed from Bowtell dataset {Tothill, 2008 #89} (Fig. 1a). We next explored correlations between YB-1 and clinical outcomes using the same datasets. As expected, patients with high levels of *YBX1* mRNA (based on the lowest *p* value of the log-rank test) had shorter relapse-free survival times {Tothill, 2008 #89} (Fig. 1b). Strikingly, high levels of phospho-YB-1 strongly predicted a poor outcome for ovarian cancer patients, with overall, almost half of the patients with low phospho-YB-1 surviving for more than 5 years (Fig. 1b, TCGA dataset). Total YB-1 protein levels and outcomes ($p = 0.11$, analyzed from patients with low versus high levels of YB-1) were not correlated potentially due to effects of phosphorylation on post-translational stability or low antibody quality. These results make phospho-YB-1 as one of the strongest outcome predictors for ovarian cancer patients yet identified and thus prompted us to investigate the regulation and consequences of YB-1 phosphorylation.

YB-1 is a target of growth factor stimulation in cancer cells

To investigate the regulation of YB-1 phosphorylation, we examined the effects of three critical growth factors, LPA, EGF and insulin-like growth factor 1 (IGF-1) using a panel of ovarian cancer cell lines (Supplementary table 1). In most of the cell lines, LPA (3.91 ± 0.50 fold) and EGF (5.59 ± 0.89 fold) markedly increased YB-1 phosphorylation (Fig. 1c). IGF-1 (1.65 ± 0.32 fold) only modestly induced YB-1 phosphorylation in a subset of these lines. This was not due to a lack of response to IGF-1 as evidenced by marked increases in AKT phosphorylation (Fig. 1c). These growth factors had no overt effects on total YB-1 levels within 1h stimulation (Fig. 1c) and, for LPA and EGF, up to 24h in CAOV3 and SKOV3 cells (Supplementary fig. 1). We next explored the generalizability of growth factor-induced YB-1 phosphorylation across tumor lineages (Supplementary table 1). Likewise, LPA (3.71 ± 0.72 fold) and EGF (7.09 ± 2.57 fold) markedly induced YB-1 phosphorylation while IGF-1 (1.24 ± 0.25 fold) had little effect (Fig. 1d). Together, these data indicate that YB-1 is a target of LPAR and EGFR activation.

Mechanisms underlying growth factor-induced YB-1 phosphorylation

Previous studies have proposed p90RSK (readout of RAS/MAPK pathway activation) and AKT as potential regulators of YB-1 phosphorylation {Basaki, 2007 #85}. We found that LPA, EGF and IGF-1 had markedly different effects on p90RSK and AKT phosphorylation across cell lineages (Fig. 1 c and d). LPA induced phosphorylation of p90RSK (2.13 ± 0.18 fold) and AKT (1.74 ± 0.32 fold). EGF also induced phosphorylation of p90RSK (3.17 ± 0.40 fold) and AKT (3.71 ± 0.99 fold). IGF-1 markedly activated AKT (5.39 ± 1.86 fold), however, did not alter phosphorylation of p90RSK (1.01 ± 0.11 fold). These growth factors

had no overt effects on total RSK1 and AKT levels within 1h stimulation. Since IGF-1 was ineffective on p90RSK and YB-1 phosphorylation, we postulated the dominant role of RAS/MAPK/p90RSK cascade on YB-1 regulation. Consistently, LPA efficiently induced YB-1 but not AKT phosphorylation in cell lines such as CAOV3, OVCAR5, CAL27, DU145 and HCC1954 (Fig 1c and d). In addition, the correlation of phospho-YB-1 with phospho-p90RSK induced by EGF (Spearman's $\rho = 0.54$, $p = 0.03$) was significantly greater than that with phospho-AKT (Spearman's $\rho = -0.06$, $p = 0.81$) analyzed from all cell lines.

Next, we used high-throughput and unbiased reverse phase protein arrays (RPPA) to identify correlations between YB-1 phosphorylation and activation of signaling pathways. SKOV3 cells, which produce and express modest levels of endogenous LPA and LPARs {Eder, 2000 #90;Fang, 2004 #112}, were stimulated with exogenous LPA over a detailed time course. The phosphorylation events induced by LPA segregated into three main groups on unsupervised cluster analysis. LPA induced a rapid and transient phosphorylation of MEK, p44/42MAPK as well as AKT (at threonine-308 and serine-473) and NF-κB (Fig. 2a, Cluster 1a and b). This was followed by delayed and more persistent phosphorylation of members of the PI3K/AKT and RAS/MAPK pathways (Fig. 2a, Cluster 2). Other phosphorylated signaling nodes by LPA include EGFR at tyrosine-992 and -1173 and SRC in a biphasic manner, first within 30 minutes and later between 4 and 24 hours after stimulation (Fig. 2a, Cluster 3a), as well as IGF-1 receptor (IGF1R) and human epidermal growth factor receptor (HER)-2 in a sustain manner (Fig 2a, Cluster 3b).

Importantly, the time course of YB-1 phosphorylation correlated with p90RSK (Fig 2a, Cluster 2) but not AKT phosphorylation. YB-1 phosphorylation also temporally paralleled that of RB, S6, p70S6K and BAD downstream of the MAPK and/or AKT pathways depending on the ligands and cellular context {Fang, 1999 #116;Lu, 2011 #61}. The time-dependent effects of LPA on YB-1 phosphorylation were confirmed by Western blotting in SKOV3 cells (Supplementary fig. 1). The relatively high basal YB-1 phosphorylation in SKOV3 cells could be due to constitutive activation of LPAR {Eder, 2000 #90;Fang, 2004 #112}.

To determine whether MEK and p90RSK activation were required for YB-1 phosphorylation, we developed an additional RPPA dataset using CAOV3 cells treated with inhibitors of MEK1/2, GSK1120212 {Jing, 2012 #71}, and RSK1/2, SL0101 {Smith, 2005 #72}. GSK1120212 abolished LPA- and EGF-induced phosphorylation of p44/42MAPK, p90RSK and S6 at 1h stimulation establishing these proteins as being downstream of MEK1/2 upon stimulation (Fig. 2b). SL0101 selectively inhibited the effects of LPA and EGF on phosphorylation of S6 but not on phosphorylation of p90RSK itself or the upstream p44/42MAPK. Importantly, inhibition of MEK1/2 or RSK1/2 suppressed both LPA- and EGF-induced YB-1 phosphorylation as shown by RPPA (Fig. 2b) or Western blotting (Supplementary fig. 2). Thus, YB-1 phosphorylation requires an intact MEK/p44/42MAPK/p90RSK pathway.

We directly determined the role of AKT using two potent AKT inhibitors with distinct actions—a catalytic domain inhibitor, GSK690693 {Rhodes, 2008 #66}, and an allosteric inhibitor, MK2206 {Hirai, 2010 #75}, in UPN and SKOV3 cells, which showed appreciable

AKT and YB-1 phosphorylation upon growth factor stimulation (Fig. 1c, 2c and Supplementary fig. 3). GSK690693 increased basal and growth-factor-induced AKT phosphorylation due to blocking a negative feedback loop downstream of AKT, while MK2206 abolished both basal and growth-factor-induced AKT phosphorylation {Cherrin, 2010 #59}. Inhibition of the AKT pathway modestly decreased S6 phosphorylation compatible with a predominant role of MAPK pathway and subsequent downstream activation (see Fig. 2b). Strikingly, neither GSK690693 nor MK2206 altered YB-1 phosphorylation induced by LPA or EGF in UPN (Fig. 2c) and SKOV3 cells (Supplementary fig. 3).

Further, we used cell lines that lack AKT to examine the effects of LPA and EGF on YB-1 phosphorylation. Deletion of *AKT1* and *AKT2*, the only AKT isoforms expressed in DLD1 and HCT116 colon cancer cells {Ericson, 2010 #60}, resulted in a complete loss of AKT and phospho-AKT under basal and activation conditions (Fig. 2d). However, both LPA and EGF could induce YB-1 phosphorylation in these cells. Together, the data argue that YB-1 phosphorylation is dependent on LPA- or EGF-induced activation of the p44/42MAPK/p90RSK pathway and not AKT.

LPA rapidly induces activation of the p44/42MAPK/p90RSK/YB-1 pathway via SRC-mediated crosstalk with the EGFR

Our RPPA analyses suggested that LPA could activate receptor tyrosine kinases including the EGFR (tyrosine-992 and -1173 phosphorylation), HER2 and IGF1R (Fig. 2a). Given the inability of IGF-1 to induce YB-1 phosphorylation, we thus placed the focus on the role of crosstalk between LPAR and the EGFR/ERBB family. Using an EGFR/ERBB phosphorylation array, we found that LPA induced EGFR phosphorylation at tyrosine-845 (~2 folds, not on the RPPA platform) in CAOV3 cells, but not phosphorylation of other ERBB receptors including HER2 (Fig. 3a). LPA also induced EGFR phosphorylation at tyrosine-845 in SKOV3 cells (see Fig. 3f, below) consistent with the role of SRC in LPA-induced EGFR transactivation {Andreev, 2001 #117}. The discrepancy on HER2 phosphorylation between this array and RPPA is likely due to the greater sensitivity of RPPA.

We next examined the EGFR as a putative link between LPAR and YB-1. Indeed, gefitinib, which is selective for EGFR {Wakeling, 2002 #80} and lapatinib, which inhibits EGFR and HER2 {Rusnak, 2001 #73} abolished not only EGF- but also LPA-induced activation of the p44/42MAPK/p90RSK/YB-1 pathway (Fig. 3b). The monoclonal antibody Cetuximab that inhibits EGFR dimerization {Talavera, 2009 #63} also blocked YB-1 phosphorylation induced by EGF and LPA (Fig. 3c). In contrast, the HER2 antibody, Trastuzumab, was not sufficient to block LPA- and EGF-induced activation of the p44/42MAPK/p90RSK/YB-1 pathway (Supplementary fig. 4). It was formally possible that EGFR activation initiates a crosstalk with the LPAR in ovarian cancer cells {Snider, 2010 #107}. We ruled out this possibility since Ki16425, an LPAR1/3 antagonist {Ohta, 2003 #65} selectively suppressed LPA but not EGF effects on the p44/42MAPK/p90RSK/YB-1 pathway (Fig. 3d).

We also demonstrated crosstalk between LPAR and EGFR in SKOV3 cells, in which activation of the p44/42MAPK/p90RSK/YB-1 pathway by EGF and LPA was inhibited by

gefitinib or lapatinib (Fig. 3e). As a site for SRC phosphorylation {Tice, 1999 #88}, LPA-induced EGFR phosphorylation at tyrosine-845 was completely inhibited by dasatinib, a dual SRC/ABL kinase inhibitor {Lombardo, 2004 #74} (Fig. 3f). Further, dasatinib selectively blocked LPA but not EGF-induced activation of the p44/42MAPK/p90RSK/YB-1 pathway (Fig. 3g) suggesting that SRC is interposed between the LPAR and the EGFR and not required for EGF-induced activation of the pathway.

LPA induces delayed AREG release that initiates a self-reinforcing loop of YB-1 phosphorylation and subsequent AREG production

Activation of SRC by GPCRs can lead to EGFR transactivation via rapid shedding of EGFR ligands from the cell surface {Zhang, 2006 #98}. We tested this possibility, in which shedding of EGFR ligands (i.e., AREG, EGF and transforming growth factor-α or TGFα) contributed to LPA-induced YB-1 phosphorylation. As expected, EGFR ligands strongly induced phosphorylation of the p44/42MAPK/p90RSK/YB-1 pathway, which was abrogated by the neutralizing antibodies (Fig. 4a). However, none of the antibodies altered the initial phase of LPA-induced phosphorylation of p44/42MAPK/p90RSK/YB-1 pathway, at the 1h time point assessed. It is likely that the initial step in LPA-mediated EGFR transactivation does not involve shedding of these EGFR ligands but is rather due to SRC activation.

LPA promotes release of cytokines and angiogenic factors from ovarian cancer cells {Fang, 2004 #112;Yu, 2008 #103}, which may include ligands for EGFR family members. In contrast to the initial signaling events, production of these EGFR ligands could contribute to the delayed phase of EGFR activation (see Fig. 2a). We first examined the levels of three EGFR ligands in supernatants of ovarian cancer cell lines. These cell lines constitutively released AREG (except HEY cells) and lower levels of TGFα ($p = 0.112$; AREG vs. TGFα) but surprisingly not EGF (Supplementary fig. 5). Within 24h of addition, LPA increased AREG levels in the supernatants of several cell lines, reaching statistical significance in CAOV3, OV2008 and SKOV3 cells (Fig. 4b) consistent with the delayed EGFR and prolonged YB-1 activation of these cells shown above. LPA did not induce EGF or increase TGFαrelease (Supplementary fig. 6). The delayed release of AREG induced by LPA could be due to upregulation of *AREG* expression. Indeed, AREG release induced by LPA was markedly reduced by cycloheximide, an inhibitor of mRNA translation (Fig. 4c). Further, LPA massively induced *AREG* mRNA expression (Fig. 4d). Unexpectedly, we also found that exogenous AREG induced *AREG* mRNA expression consistent with LPA initiating a self-reinforcing loop involving production and release of AREG, which in turn, upregulates its own production.

It is plausible that the newly produced AREG initiates the delayed component of biphasic EGFR activation and contributes to prolonged YB-1 activation induced by LPA. Indeed, the AREG neutralizing antibody significantly suppressed delayed YB-1 phosphorylation from 4 to 24h following LPA addition, while it had no effect within the first 2h (Fig. 4e). In contrast, both initial and delayed effects were completely inhibited by gefitinib in keeping with the requirement of LPAR/EGFR crosstalk for initial activation of YB-1. AREG release by LPA but not EGF was sensitive to SRC inhibition, while AREG release by both LPA and EGF was sensitive to EGFR and MEK1/2 inhibition (Fig. 4f and g). These data suggest that

YB-1 phosphorylation and AREG release by LPA involve two phases of EGFR activation and the delayed AREG release is required for prolonged activation of the p44/42MAPK/p90RSK/YB-1 pathway.

YB-1 is critical for LPA-induced AREG release and cell invasion through the EGFR crosstalk and activation of the p44/42MAPK/p90RSK pathway

We then asked whether the AREG autoregulatory loop was dependent on YB-1 activation by examining the role of YB-1 in cytokine production. LPA induced at least a two-fold increase in levels of AREG, glial cell line-derived neurotrophic factor, coagulation factor III and CD26 but not EGF and HB-EGF in supernatants assessed by cytokine array (Fig. 5b and Supplementary table 2). Importantly, *YBX1* knockdown markedly decreased LPA-induced AREG release as assessed using the array and confirmed by ELISA (Fig. 5c). These findings suggest a self-reinforcing loop of AREG and YB-1, in which AREG is released initially upon YB-1 phosphorylation and subsequently acts as a mediator of YB-1 phosphorylation.

LPA and EGF are critical mediators of cell mobility and invasion. We thus explored the role of YB-1 in cell invasion. *YBX1* knockdown significantly inhibited LPA-induced invasion of SKOV3 cells (Fig. 5d). Further, inhibition of the EGFR abolished both EGF- and LPA-induced invasion of SKOV3 cells (Fig. 5e) supporting the importance of proposed signaling pathway. The effects of LPA and EGF on cell invasion were also sensitive to MEK1/2 and RSK1/2 but not AKT inhibition (Supplementary fig. 7 and 8) in keeping with the role of p44/42MAPK/p90RSK pathway in YB-1 phosphorylation. Together, our data consistently indicate that activation of YB-1 through LPAR/EGFR crosstalk and p44/42MAPK/p90RSK pathway contributes to functional outcomes including AREG release and ovarian cancer cell invasion (Fig. 5f).

The EGFR crosstalk and AREG/YB-1 self-reinforcing loop mediate LPA-induced tumor growth and aggressiveness *in vivo*

We found that high levels of *EGFR* expression predicted a poor outcome with lowered survival fraction using TCGA dataset ($p = 0.0059$, Supplementary figure 9) thus this warrants the EGFR as therapeutic target in ovarian cancer. Although, there was no significant correlation between *LPAR2* levels and the survival fraction in this dataset ($p = 0.15$, Supplementary figure 9), we have shown that ectopic expression of LPAR enhances growth of SKOV3 cells through an autocrine LPA signaling loop {Yu, 2008 #103}. Therefore, we further evaluated the significance of proposed signaling pathway using this xenograft model. Indeed, enforced LPAR2 expression in SKOV3 cells (SKOV3-LPAR2) results in significantly greater collective weights of tumors that attached to abdominal organs, omentum and peritoneal membrane compared to those of β-galactosidase-expressing cells (SKOV3-LacZ) as control (Fig. 5g). Inhibition of LPAR/EGFR crosstalk with gefitinib markedly decreased growth of SKOV3-LPAR2 tumors, with the collective weights of treated tumors being comparable to those of SKOV3-LacZ tumors. Histological analyses also revealed a significant decrease in tumor invasiveness with gefitinib (Supplemental figure 10). Importantly, mice bearing SKOV3-LPAR2 tumors also showed elevated serum AREG with increased phosphorylated YB-1 levels in the tumors (Fig. 5h and i). These increases were also effectively blocked by gefitinib. Therefore, these findings recapitulate

the signaling pathway developed *in vitro*, wherein LPA induces EGFR transactivation leading to YB-1 phosphorylation and subsequent AREG production in ovarian tumors.

DISCUSSION

In this study, we have uncovered the regulation and function of YB-1 in ovarian cancer using clinical data, high-throughput arrays with complementary biochemical methods and an ovarian xenograft model. We reveal here that YB-1 is a novel and generalized target of LPA and EGF signaling across cancer types. Further, high levels of phospho-YB-1, presumably due to activation of growth factor signaling, are associated with poor outcomes in ovarian cancer patients. These further establish YB-1 as a critical oncogenic factor that drives aggressiveness of tumors in human and mice as previously proposed in breast cancer {Bergmann, 2005 #100}. Our study points to an increase in ovarian cancer cell invasiveness as a potential cause of the worsened outcomes concordant with an increase in metastatic potential of breast cancer cells observed with overexpression of YB-1 {Evdokimova, 2009 #87}. In ovarian cancer, increased nuclear expression of YB-1 is also associated with outcomes and the resistance to chemotherapy {Basaki, 2007 #85;Yahata, 2002 #86}. Therefore, our present study uncovers the mechanism and significance of YB-1 phosphorylation that could lead to the development of effective regimens to improve outcomes for ovarian cancer and potentially for tumors of other lineages.

AKT and p90RSK were proposed to phosphorylate YB-1 in basal breast cancer cell lines {Stratford, 2008 #102}. However, the mechanisms by which these kinases regulate YB-1 were not well defined. Here, we provide conclusive evidence that LPA- and EGF-induced YB-1 phosphorylation is predominantly regulated via the p44/42MAPK/p90RSK pathway and not the AKT pathway in the broad range of cells studied. The p44/42MAPK/p90RSK pathway coordinates functional outcomes including AREG production and cell invasion in our study as well as gene expression in colorectal cancer cells {Jurchott, 2010 #70}. Targeting this pathway may have a therapeutic implication as implicated in the xenograft model of ovarian cancer and triple-negative breast cancer {Stratford, 2012 #64}. While our data excluded the involvement of AKT, AKT has been proposed in nuclear translocation of YB-1 and associated with aggressiveness of ovarian cancer cells {Basaki, 2007 #85}. It is possible that there is an alternative and yet unidentified AKT-dependent pathway that regulates YB-1 nuclear localization in ovarian cancer.

YB-1 has been proposed to support tumor growth through activation of EGFR signaling independent of exogenous EGF {Berquin, 2005 #84;Wu, 2006 #83}. Indeed, present study reveals a plausible mechanism of EGFR autoregulation specifically via AREG production. Endogenous AREG can form a self-reinforcing loop of YB-1 activation and further production of AREG. The significance of the autoregulation has been shown wherein AREG acts as an essential autocrine growth factor that promotes growth of mammary tumors {Berquin, 2001 #96;Normanno, 1994 #97}. Our data also revealed that ovarian cancer cell lines constitutively produce AREG at higher levels compared to EGF and TGFα suggesting that AREG is a critical and relevant EGFR ligand that promotes ovarian cancer progression.

In the proposed signaling pathway, EGFR activation occurs through two distinct and temporally independent mechanisms, an initial transactivation induced by SRC followed by delayed activation of the EGFR through YB-1-dependent upregulation of *AREG*. While we found that SRC-mediated shedding of AREG to be the underlying mechanism of EGFR crosstalk in head-and-neck cancer cells {Zhang, 2006 #98}, the initial phase of EGFR crosstalk was found to be dependent on SRC but independent of AREG shedding in ovarian cancer cells. Thus, crosstalk between GPCRs (LPAR in ovarian cancer and gastrin-releasing peptide receptor in head-and-neck cancer) and receptor tyrosine kinases (EGFR) can occur through diverse mechanisms as previously proposed {Rodland, 2008 #108}.

The delayed production of AREG may explain the need for prolonged exposure to LPA and consequent SRC-mediated EGFR phosphorylation and p42/44 MAPK activation to induce DNA synthesis and cellular proliferation {Cook, 1996 #76;Boerner, 2005 #113}. In addition, we have reported that the LPAR/EGFR transactivation enhanced MMP-9 expression and invasiveness of ovarian cancer cells via RAS/Rho/ROCK/NF-κB pathway {Jeong, 2013 #118}. It is possible that both phases of EGFR activation are required for LPA-induced ovarian tumor growth and aggressiveness as observed in ovarian xenograft tumors driven by LPA2 receptors. Interestingly, our preliminary data in SKOV3 cells suggested that MMP-9 release by LPA was less effective when *YBX1* was knockdown (Supplementary table 2). Therefore, the ongoing AREG/YB-1 autoregulation may require for maintaining optimal EGFR activation. While we have revealed the pathway that initiates AREG/YB-1 self-reinforcing loop, the mechanism by which this loop is terminated remains to be ascertained. It likely involves an induction of phosphatases such as the dual specific phosphatases, which are the components of negative feedback pathway that regulates EGFR/MAPK activation {Amit, 2007 #77}.

LPA receptors represent potential therapeutic targets with a number of approaches being under investigation {Panupinthu, 2010 #109} and several EGFR inhibitors have already been approved for use, albeit with limited activity as single agent. Inhibition of GPCRs or SRC can increase the sensitivity of tumor cells to anti-EGFR targeted therapy {Li, 2009 #93;Zhang, 2007 #92}, potentially by interrupting the crosstalk and self-reinforcing AREG loop. However, the limited effects of the EGFR inhibitors in ovarian cancer should be interpreted with caution since resistance can occur rapidly and limit the efficacy {Siwak, 2010 #91}. Based on our current work, the mechanisms of resistance could involve the initiation of the AREG/YB-1 self-reinforcing loop. Indeed, resistance to gefitinib could be overcome by knockdown of *AREG* {Busser, 2010 #94}. Our data also argue that YB-1 is an interesting therapeutic target since it acts as integration point of EGFR activation via crosstalk and autoregulation. In this regard, small molecules targeting YB-1 phosphorylation has been developed {Law, 2010 #95} and could alleviate resistance to EGFR therapy. In summary, there are a number of plausible regimens targeting multiple steps of an important signaling pathway for the pathophysiology of ovarian cancer that might improve outcomes in patients. These coordinate inhibition approaches may demonstrate favorable efficacy and thus warrant further exploration.

MATERIALS AND METHODS

Cell lines and reagents

Ovarian, prostate and breast cancer cell lines and MCF10A cells were from the Characterized Cell Line Core Facility of the MD Anderson Cancer Center. Head-and-neck cancer cell lines were from ATCC (Manassas, VA). Lung cancer cell lines were from Dr. John Heymach at MD Anderson Cancer Center. Colon cancer cells were from Dr. Bert Vogelstein at Johns Hopkins Kimmel Cancer Center. Cell lines were authenticated by STR screening and confirmed to be mycoplasma-negative by the Cell Line Core Facility and maintained in a complete medium (RPMI-1640 or DMEM containing 5% fetal bovine or horse serum). IGF-1, EGFR ligands and the neutralizing antibodies were from R&D Systems (Minneapolis, MN). LPA (1-oleoyl-2-hydroxy-*sn*-glycero-3-phosphate) and Ki16425 were from Avanti Polar Lipids Inc (Alabaster, AL). Cetuximab and Trastuzumab were from pharmacy at the MD Anderson Cancer Center. GSK1120212 was obtained under a material transfer agreement with GlaxoSmithKline (Boston, MA). SL0101 was from EMD Millipore (Billerica, MA). Gefitinib and lapatinib were from LC Laboratories (Woburn, MA). GSK690693, MK-2206 and dasatinib were from Selleck Chemicals LLC (Houston, TX). Growth factors were prepared in phosphate buffered saline containing 1 mg/ml of fatty acid-free bovine albumin. All inhibitors were dissolved in dimethyl sulfoxide.

Datasets of ovarian cancer patients

Two datasets of ovarian cancer patients (TCGA and Bowtell datasets) were included in the analyses without the restriction of stage or age. In TCGA dataset, YBX1 expression was analyzed from 519 ovarian serous cystadenocarcinoma samples and 8 unmatched normal ovarian tissue samples. There were 332 serous cystadenocarcinoma samples with matched RPPA data and outcomes. These samples were from patients with stage II (5.1%), stage III (80.4%) and stage IV (14.9%) tumors and age range of 27.2 to 84.7 years. In Bowtell dataset, 267 samples were characterized as high-grade, late-stage serous ovarian tumors and 18 samples were characterized as low-grade, early-stage ovarian tumors with low malignant potential. For further information, see Table 1 of the original paper by Tothill and coworkers {Tothill, 2008 #89}.

Antibody arrays, Western blot analyses and ELISA

RPPA was performed in triplicate samples of CAOV3 and SKOV3 cells as described previously {Zhang, 2009 #101}. Heat map with hierarchical clustering using the normalized levels of phospho-proteins was obtained using Cluster 2.11 {Eisen, 1998 #58}. Western blots were performed as previously described {Yu, 2008 #103}. All antibodies are listed in Supplementary table 3. We assessed EGFR/ERBB phosphorylation profile using human EGFR phosphorylation antibody array (RayBiotech, Inc., Norcross, GA). Production of cytokines was assessed using a human angiogenesis antibody array or DuoSet ELISA kits (R&D Systems, Minneapolis, MN). Band and spot intensities were quantified using AlphaView SA version 3.2.3.0 (ProteinSimple, Santa Clara, CA).

RNA-interference knockdown

Two individual small interference RNAs targeting *YBX1* (siYBX1 #1, GGCGAAGGUUCCCACCUUA and siYBX1 #2, CGGCAAUGAAGAAGAUAAA) and non-silencing control (siControl) were obtained from Cell Signaling Technology, Inc (Danvers, MA). The siRNAs were delivered into cells using Lipofectamine RNAiMAX reagent (Life Technologies, Grand Island, NY).

Transwell migration and invasion assay

Cells were seeded on Matrigel-coated transwell invasion chambers with 8-m pore size (BD Bioscience, San Jose, CA) at 5×10^4 cells in serum-free medium containing inhibitors. The chambers were then placed into each well of the 24-well plate containing serum-free medium with growth factors. After 24h incubation, invasive cells were visualized using crystal violet and counted.

Real-time RT-PCR

Real-time RT-PCR was performed using the ABI Prism 7900 HT Sequence Detector (PerkinElmer, Waltham, MA) and samples were processed as described previously {Yu, 2008 #103}.

Mouse xenograft model of SKOV3 cells overexpressing LPA2 receptors

SKOV3 cells expressing lentiviral constructs carrying *LPAR2* or *LacZ* gene were injected intraperitoneally into six-week-old BALB/c Nu/Nu female mice as described previously {Yu, 2008 #103}. In both groups, mice were randomly divided to receive gefitinib (100 mg/kg) or vehicle orally one week after tumor cell injection. The animals were then treated every three days for an additional two weeks and euthanized. Tumor burden was measured as a collective weight of all visible nodules that attached to abdominal organs, omentum and peritoneal membrane of stomach wall. Protein from tumors was extracted for Western blots. Blood samples were collected and serum levels of AREG were assessed using ELISA. Histological procedures were performed as described previously {Yu, 2008 #103}. M. Gagae scored invasiveness of the tumors according to the criteria in Supplemental table 4. All procedures were conducted in compliance with the regulations of MD Anderson Cancer Center Institutional Animal Care and Use Committee.

Statistical Analyses

Box-and-whisker diagrams indicate means and SD. Bar graphs indicate means ± SEM. We estimated overall survival durations of ovarian cancer patients non-parametrically using Kaplan– Meier curves. Log-rank tests were conducted to compare overall survival durations between patients with high (>0) versus low (≤0) level of *YBX1* expression or phospho-YB-1. The correlation between levels of phospho-proteins was determined using Spearman's rank correlation coefficient. Differences between two groups were assessed using two-sided Student's *t* tests. Differences among three or more groups were evaluated by one-way ANOVA followed by a Dunnett's multiple comparisons test, or two-way ANOVA followed by a Bonferroni multiple comparisons test. Data were analyzed by GraphPad Prism version 5.0. Differences were accepted as statistically significant at $p < 0.05$.

Supplementary Material

Refer to Web version on PubMed Central for supplementary material.

Acknowledgments

We thank Meng Gao and Dr. Zhiyong Ding at MD Anderson Cancer Center for authenticating the *AKT1*/*AKT2* knockout cell lines. This work was supported by NIH grants R01CA92160 and P01CA099031 (to G.B.M.), and R01CA098372 (to J.R.G.), the Breast Cancer Research Foundation (to G.B.M.), the National Research Foundation of Korea 2011-0015761 (to H.Y.L.), Canadian Institutes of Health Research (to S.E.D.), the SPORE in head-and-neck cancer P50CA197190 (to J.R.G.), the American Cancer Society (to J.R.G.) and CCSG core grant CA16672 (to MD Anderson Cancer Center).

ABBREVIATIONS

AREG	Amphiregulin
EGFR	Epidermal growth factor receptor
GPCR	G-protein-coupled receptor
HER	human epidermal growth factor receptor
IGF-1	insulin-like growth factor 1
IGF1R	insulin-like growth factor 1 receptor
LPA	lysophosphatidic acid
LPAR	lysophosphatidic acid receptor
p90RSK	p90 ribosomal S6 kinase
PI3K	phosphatidylinositol 3-kinase
RPPA	reverse phase protein array
TCGA	The Cancer Genome Atlas
TGFα	transforming growth factor-α
YB-1	Y-box binding protein-1

REFERENCES

1. Panupinthu, Nattapon; Zhang, Dong; Zhang, Fan; Gagae, Mihai; Mills, Gordon B. Department of Systems Biology, The University of Texas MD Anderson Cancer Center; Houston, TX, 77030, USA:
2. Lu, Yiling. Department of Veterinary Medicine & Surgery, The University of Texas MD Anderson Cancer Center; Houston, TX, 77030, USA:
3. Yu, Shuangxing. Department of Physiology, Faculty of Science, Mahidol University; Bangkok, 10400, Thailand:
4. Grandis, Jennifer R. Department of Otolaryngology and Department of Pharmacology and Chemical Biology, University of Pittsburgh; Pittsburgh, PA, 15213, USA:
5. Dunn, Sandra E. Departments of Pediatrics and Experimental Medicine, Child and Family Research Institute, University of British Columbia; Vancouver, BC, V5Z 4H4, Canada:
6. Young Lee, Hoi. Department of Pharmacology, College of Medicine, Konyang University; Daejeon, 302-718, Republic of Korea:

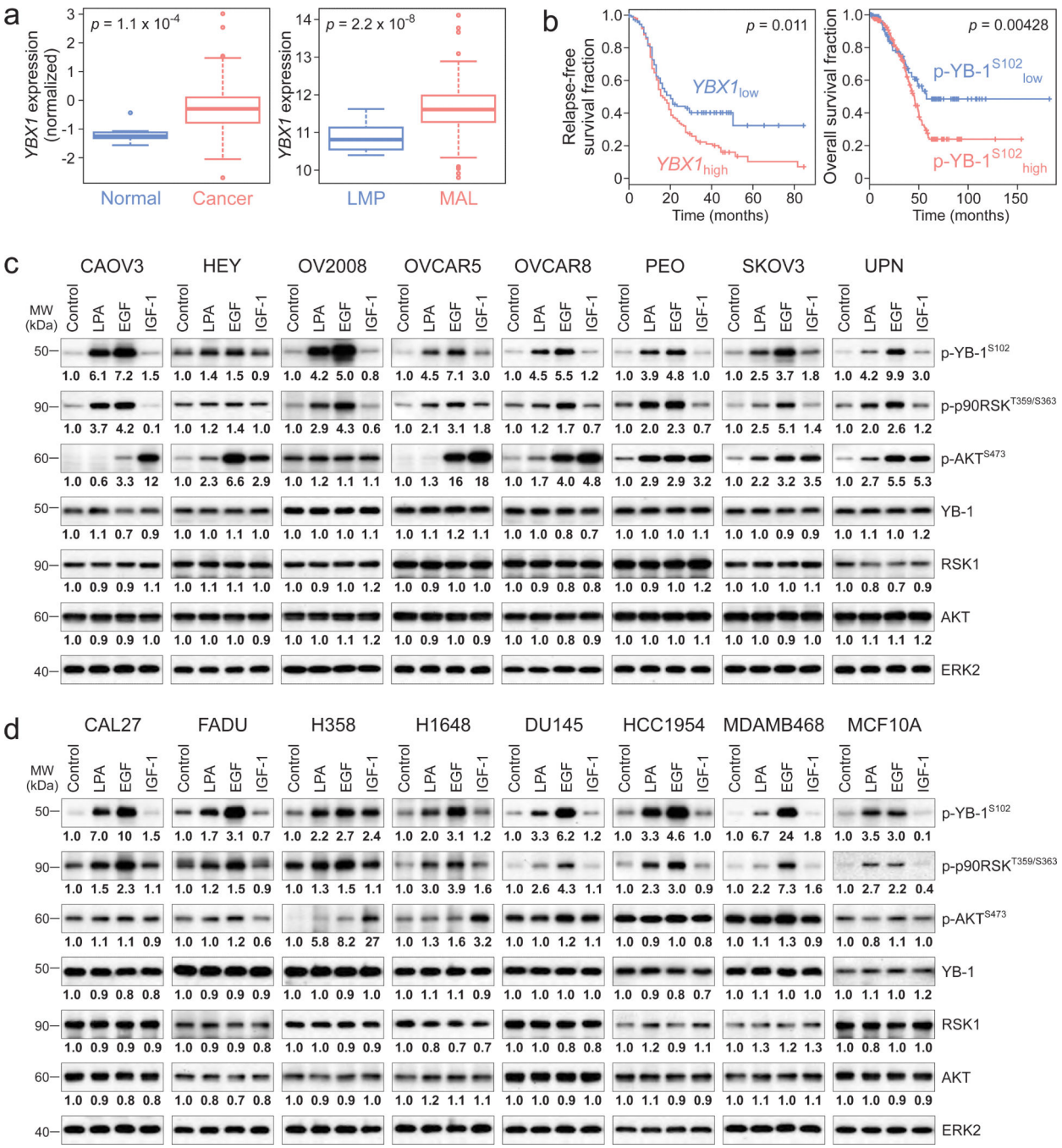

Figure 1.

Growth factors induce phosphorylation of oncogenic transcription factor YB-1 in cancer cells. (**a**) Box-and-whisker diagrams show levels of *YBX1* expression in normal (n = 8) and cancer (n = 511) samples (left panel), and in samples with low malignant (*LMP*, n = 18) and malignant (*MAL*, n = 267) potentials (right panel). Data are means ± SD. (**b**) Kaplan-Meier curves show the relapse-free or overall survival durations among ovarian cancer patients with low and high levels of *YBX1* expression ($YBX1_{low}$, n = 162 and $YBX1_{high}$, n = 113, left panel) and levels of phospho-YB-1 ($p\text{-YB-1}^{S102}{}_{low}$, n = 131 and $p\text{-YB-1}^{S102}{}_{high}$, n = 201,

right panel). The survival data for *YBX1* expression levels in **b** were censored at 84 months and *p* values are indicated for all panels. Eight ovarian cancer cell lines (**c**) and cancer cell lines of other lineages as well as non-transformed mammary epithelial MCA10A cells (**d**) were treated with LPA (10 μM), EGF (10 ng/ml) or IGF-1 (10 ng/ml) for 1h and Western blot was performed. Band intensities of phospho-YB-1 (p-YB-1^{S102}), phospho-p90RSK (p-p90RSK$^{T359/S363}$), phospho-AKT (p-AKT^{S473}), YB-1, RSK1 and AKT were quantified and normalized to the intensity of ERK2. Micrographs are representative of three independent preparations.

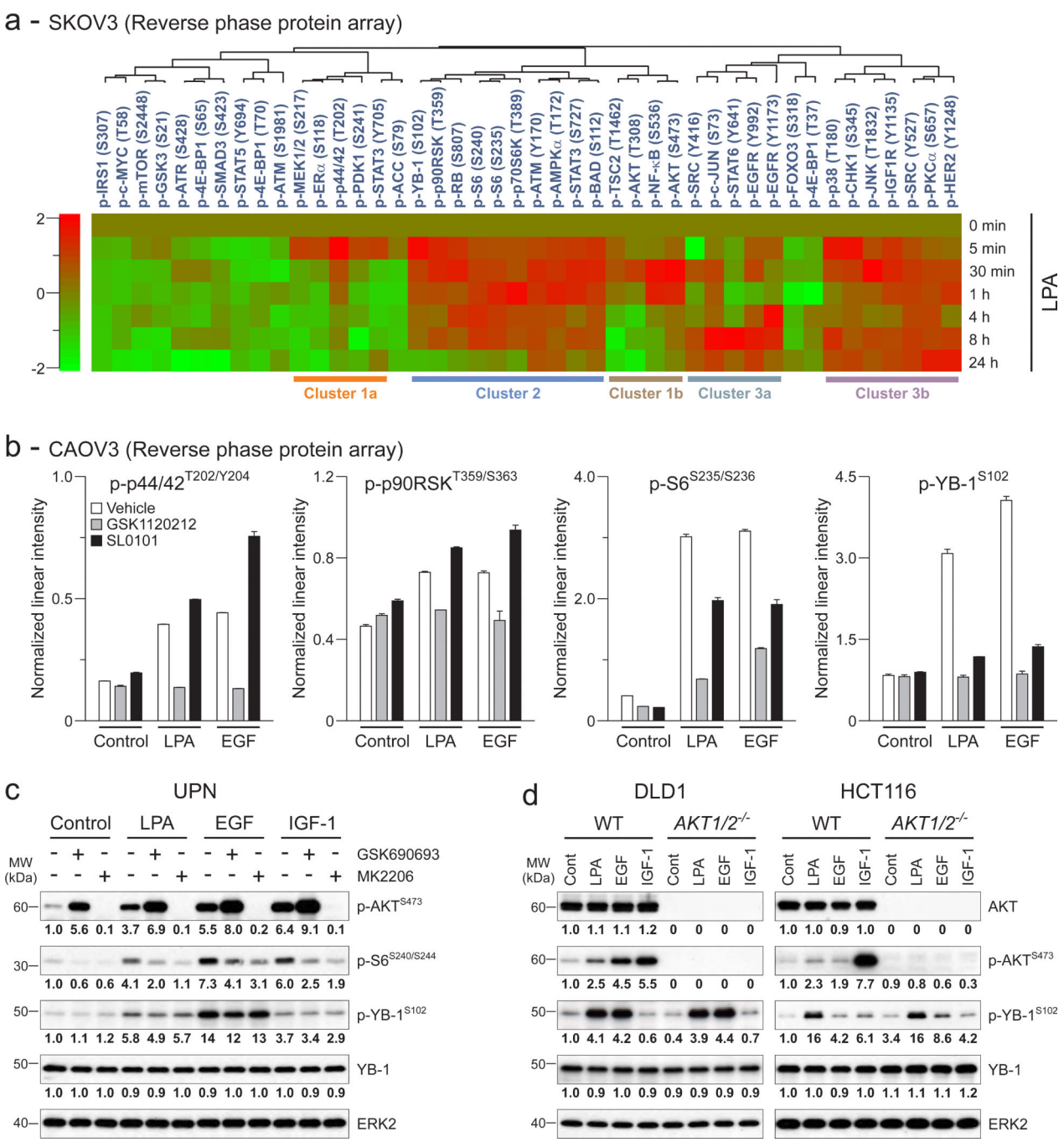

Figure 2.

LPA and EGF induce YB-1 phosphorylation through p44/42MAPK/p90RSK but not AKT pathway (**a**) Heat map depicts average intensities of phospho-proteins from RPPA and unsupervised cluster analyses in SKOV3 cells treated with LPA (10 μM) as time indicated. Changes in the average intensities were normalized to start. The color range is indicated on left. (**b**) In another set of RPPA, CAOV3 cells were treated with GSK1120212 (1 μM) or SL0101 (100 μM) for 1h followed by LPA (10 μM) or EGF (10 ng/ml) for another 1h. Data are means ± SEM of triplicate samples. (**c**) UPN cells were treated with GSK690693 or

MK2206 (1 μM) for 1h followed by LPA (10 μM), EGF or IGF-1 (10 ng/ml) for another 1h and Western blot was performed. Band intensities of phospho-AKT (p-AKT^{S473}), phospho-S6 (p-S6$^{S240/S244}$), phospho-YB-1 (p-YB-1^{S102}) and YB-1 were quantified and normalized to the intensity of ERK2. (**d**) DLD1 and HCT116 cells (WT and *AKT1/2*$^{-/-}$) were treated with LPA (10 μM), EGF or IGF-1 (10 ng/ml) for 1h and Western blot was performed. Band intensities of AKT, p-AKT^{S473}, p-YB-1^{S102} and YB-1 were quantified and normalized. Micrographs are representative of three independent preparations.

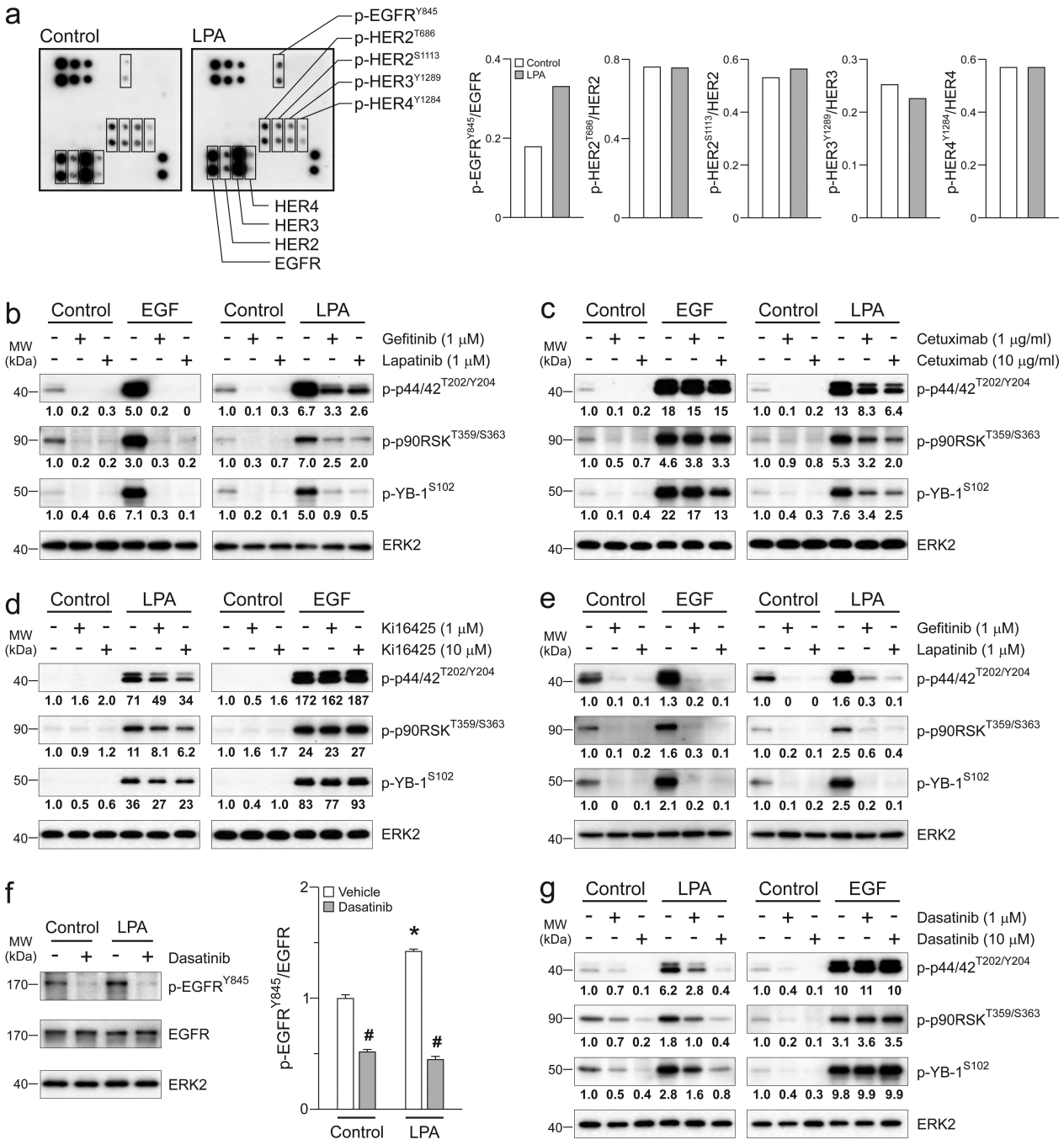

Figure 3.

LPA induces activation of p44/42MAPK/p90RSK/YB-1 pathway through SRC-mediated EGFR crosstalk. (**a**) CAOV3 cells were treated with LPA (10 μM) for 1h and phosphorylation levels of the EGFR/ERBB receptors were assessed using human EGFR family phosphorylation antibody array. Dot intensities were quantified on right. CAOV3 cells were treated with gefitinib or lapatinib (1 μM, **b**), Cetuximab (1 or 10 μM, **c**) or Ki16425 (1 or 10 μM, **d**) for 1h followed by LPA (10 μM) or EGF (10 ng/ml) for another 1h. (**e**) SKOV3 cells were treated with gefitinib or lapatinib followed by LPA or EGF

similar to **b**. Western blot was performed in **b**-**e**. Band intensities of phospho-p44/42MAPK (p-44/42$^{T202/Y204}$), phospho p90RSK (p-p90RSK$^{T359/S363}$), phospho-YB-1 (p-YB-1^{S102}) and YB-1 were quantified and normalized to the intensity of ERK2. (**f**) SKOV3 cells were treated with dasatinib (1 μM) for 1h followed by LPA (10 μM) for another 1h and Western blot was performed (left panel). Band intensities of phospho-EGFR (p-EGFR^{Y845}) were quantified and normalized to the intensity of EGFR (right panel). Data are means ± SEM, $n = 3$ independent preparations, $^{*}p < 0.05$ compared to Control and $^{\#}p < 0.05$ compared to vehicle. (**g**) SKOV3 cells were treated with dasatinib and LPA similar to **f** and Western blot was performed with antibodies used in **b**-**e**. Western blot micrographs are representative of three independent preparations.

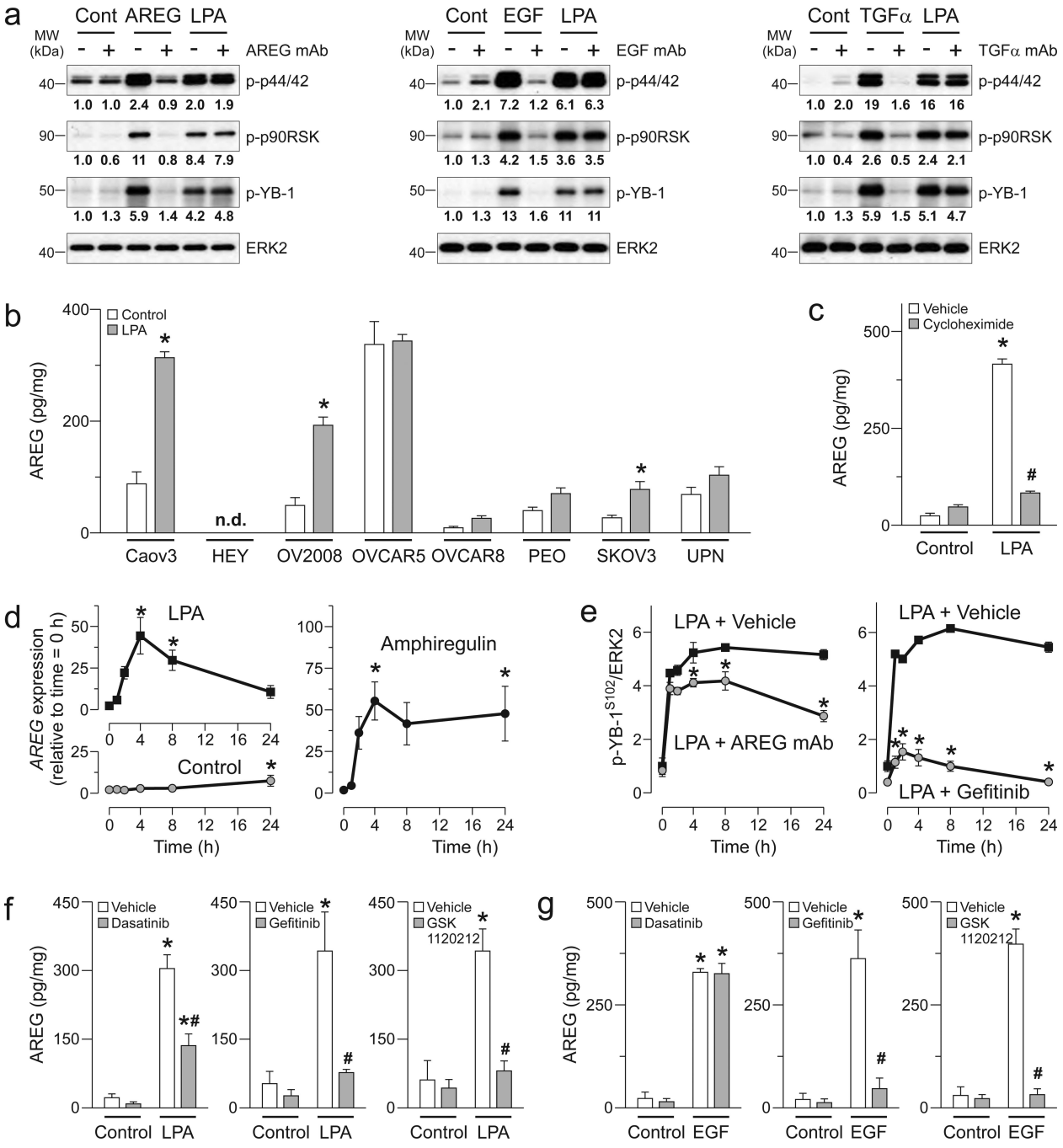

Figure 4.

LPA induces delayed YB-1 phosphorylation through autoregulation of AREG production. (**a**) CAOV3 cells were treated with neutralizing monoclonal antibodies (mAb) for AREG, EGF or TGFα (50 αg/ml) for 1h followed by the respective ligands (10 ng/ml) or LPA (10 μM) for another 1h and Western blot was performed. Band intensities of phosphop44/42MAPK (p-44/42), phospho-p90RSK (p-p90RSK), phospho-YB-1 (p-YB-1) and YB-1 were quantified and normalized to the intensity of ERK2. Micrographs are representative of three independent preparations. (**b**) Eight ovarian cancer cells were treated

with LPA (10 αM) for 24h. Supernatants were collected and levels of AREG were assessed. n.d. = not determined. (**c**) CAOV3 cells were treated cycloheximide (10 μM) for 1h followed by LPA (10 μM) for another 8h and levels of amphiregulin were assessed. (**d**) CAOV3 cells were treated with LPA (10 μM) or AREG (10 ng/ml) as times indicated and real-time RT-PCR was performed. (**e**) CAOV3 cells were treated with mAb for AREG (50 mg/ml, left panel) or gefitinib (1 μM, right panel) for 1h followed by LPA as times indicated and Western blot was performed. Band intensity of phospho-YB-1 (p-YB-1^{S102}) was quantified and normalized. Changes of p-YB-1^{S102}/ERK2 ratios are normalized to ratio of the vehicle-treated cells at start (t = 0). CAOV3 cells were treated with dasatinib, gefitinib or GSK1120212 (1 μM) for 1h followed by LPA (10 μM, **f**), EGF (10 ng/ml, **g**) for another 8h and levels of AREG were assessed. Data are means ± SEM, n = 3 independent preparations, *$p < 0.05$ compared to Control, t = 0 or LPA + vehicle and $^{\#}p < 0.05$ compared to vehicle.

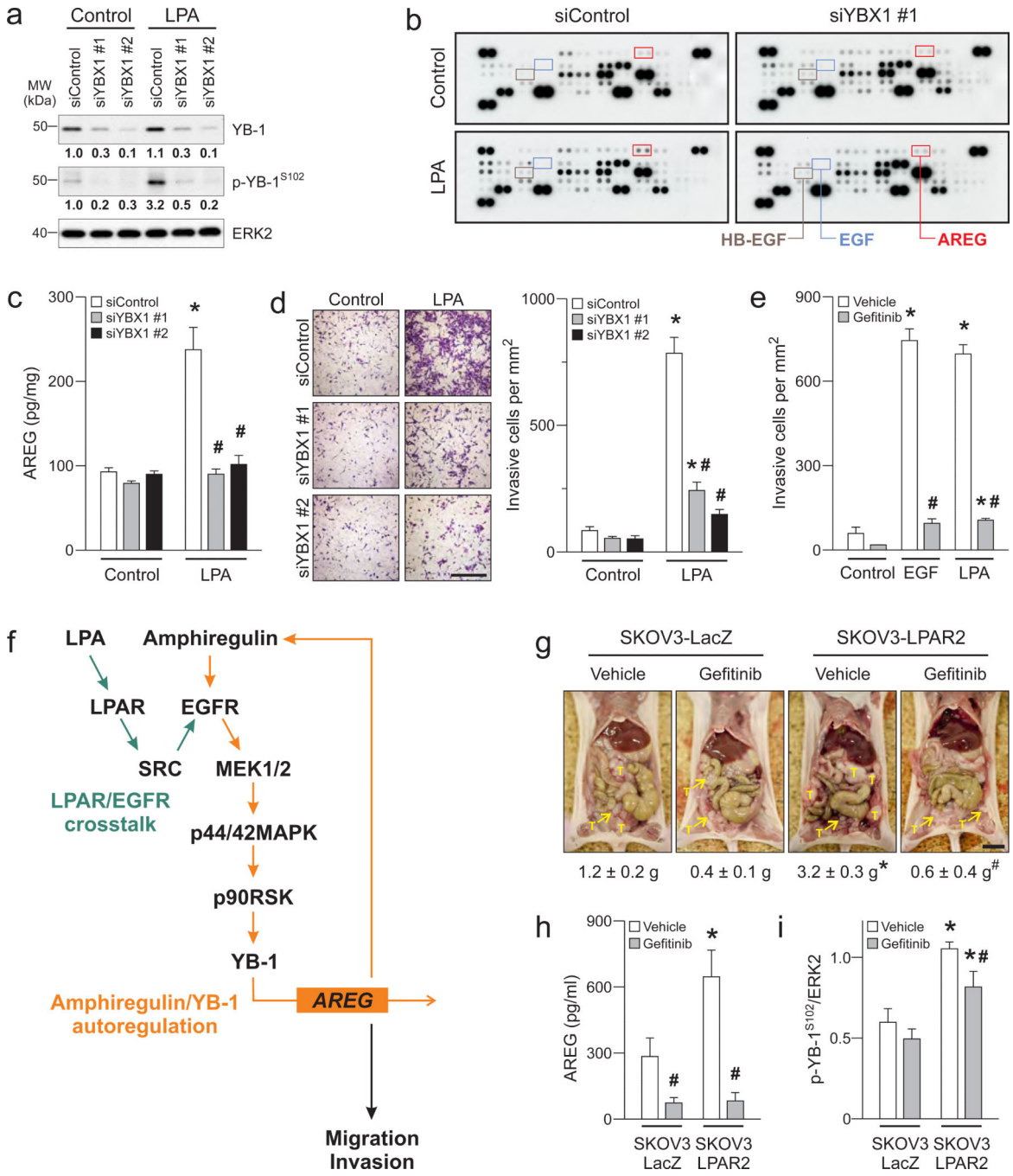

Figure 5.

Autoregulatory loop of AREG and YB-1 initiated by LPA regulates functional outcomes of ovarian cancer cells. (**a**) SKOV3 cells were treated with two *YBX1* siRNAs (siYBX1 #1 and #2) or non-silencing control (siControl) for 72h followed by LPA (10 μM) for another 1h and Western blot was performed. Band intensities of YB-1 and phospho-YB-1 (p-YB-1^{S102}) were quantified and normalized to the intensity of ERK2. Micrographs are representative of three independent preparations. SKOV3 cells with *YBX1* knockdown were treated with LPA (10 μM) for 8h and levels of cytokines and angiogenic factors (including AREG, EGF and

HB-EGF as indicated) in supernatants were assessed using human angiogenesis antibody array (**b**) and ELISA (**c**). (**d**) In transwell invasion chambers, SKOV3 cells with *YBX1* knockdown were exposed to LPA (10 μM) for 24h. Invasive cells were stained (left panel, Scale = 100 μm) and quantified (right panel). (**e**) SKOV3 cells were treated with gefitinib (1 μM) and exposed to EGF (10 ng/ml) or LPA (10 μM) for 24h. Invasive cells were stained and quantified. Data are means ± SEM, $n = 3$ independent preparations, $^{*}p < 0.05$ compared to Control and $^{\#}p < 0.05$ compared to siControl or vehicle. (**f**) Schematic diagram depicts LPA promotes migration and invasion of ovarian cancer cells through EGFR/MAPK activation and AREG/YB-1 autoregulatory loop. (**g**) All visible tumor masses (T) that attached to abdominal organs, omentum and peritoneal membrane were collected from mice injected with SKOV3-LacZ or SKOV3-LPAR2 cells and weighted. Bar is 1 cm. (**h**) Blood samples were collected and the serum levels of AREG were assessed. (**i**) Protein lysates were extracted from tumors and Western blot was performed. Band intensity of p-YB-1^{S102} was quantified and normalized to the intensity of ERK2. Data are means ± SEM, $n = 5$-8 mice per group, $^{*}p < 0.05$ compared to SKOV3-LacZ group and $^{\#}p < 0.05$ compared to vehicle.